Dang, X., Yang, H., Naafs, B. D. A., Pancost, R. D., & Xie, S. (2016). Evidence of moisture control on the methylation of branched glycerol dialkyl glycerol tetraethers in semi-arid and arid soils. *Geochimica et Cosmochimica Acta*, *189*, 24-36. https://doi.org/10.1016/j.gca.2016.06.004

Evidence of moisture control on the methylation of branched glycerol dialkyl glycerol tetraethers in semi-arid and arid soils

Xinyue Dang [a], Huan Yang [a], B. David A. Naafs [b], Richard D. Pancost [b], Shucheng Xie [a, *]

[a] *State Key Laboratory of Biogeology and Environmental Geology, School of Earth Sciences, China University of Geosciences, Wuhan 430074, China*

[b] *Organic Geochemistry Unit, Bristol Biogeochemistry Research Centre and The Cabot Institute, School of Chemistry, University of Bristol, Cantock's Close, Bristol BS8 1TS, UK*

*Author to whom correspondence should be addressed (xiecug@163.com)

Abstract

The distribution of bacterial branched glycerol dialkyl glycerol tetraethers (brGDGTs) is influenced by growth temperature and pH. This results in the widespread application of the brGDGT-based MBT(')/CBT proxy (MBT-methylation of branched tetraethers, CBT-cyclization of branched tetraethers) in terrestrial paleo-environmental reconstructions. Recently, it was shown that the amount of precipitation could also have an impact on CBT, as well as the abundance of brGDGTs relative to that of archaeal isoprenoidal (iso)GDGTs ($R_{i/b}$) and the absolute abundance of brGDGTs, potentially complicating the use of MBT/CBT as paleothermometer. However, the full influence of hydrology, and in particular soil water content (SWC), on GDGT distributions remains unclear. Here we investigated variations in the GDGT distribution across a SWC gradient (0-61%) around Qinghai Lake in the Tibetan Plateau, an arid to semiarid region in China. Our results demonstrate that SWC affects the brGDGT distribution. In particular, we show that SWC has a clear impact on the degree of methylation of C6-methylated brGDGTs, whereas C5-methylated brGDGTs are more impacted by temperature. This results in a combined SWC and temperature control on MBT'. In this context we propose a diagnostic parameter, the IR_{6ME} (relative abundance of C6-methylated GDGTs) index, to evaluate the applicability of brGDGT-based paleotemperature reconstructions. Using the global dataset, expanded with our own data, MBT' has a significant correlation with mean annual air temperature when $IR_{6ME} < 0.5$,

allowing for the use of MBT'/CBT as temperature proxy. However, MBT' has a significant correlation with mean annual precipitation (i.e., a substantial reflection of SWC impact) when $IR_{6ME} > 0.5$, implying that MBT' may respond to hydrological change in these regions and can be used as a proxy for MAP.

1. Introduction

Lipid biomarkers, including bacterial branched glycerol dialkyl glycerol tetraethers (brGDGTs) and archaeal isoprenoidal (iso)GDGTs, are widely used to reconstruct past environmental conditions in a range of environments (Schouten et al., 2002, 2013; Weijers et al., 2007; Peterse et al., 2012; De Jonge et al., 2014a). Ultimately the reliability of paleo-reconstructions depends on how well the environmental factors controlling these proxies are known in modern settings. Due to the large heterogeneity of terrestrial environments, many proxies, such as the carbon isotopes of organic matter and leaf wax lipids (Zhang et al., 2006; Bendle et al., 2007; Ning et al., 2008; Rao et al., 2013), pollen distributions (Wu et al., 2007) and phytolith distributions (Lu et al., 2006, 2007), appear to be controlled by a range of environmental factors, complicating their interpretation (e.g. ambiguity of temperature vs precipitation control). Consequently, it is necessary to develop new proxies or refine existing ones.

BrGDGTs are presumed to be the membrane-spanning lipids of as-yet unknown bacteria that likely favour anaerobic settings (Weijers et al., 2004, 2009, 2010). The occurrence of brGDGTs-Ia (Fig. 1) in some culture isolates of Acidobacteria suggests that these bacteria are likely the producers of at least one of the brGDGTs observed in natural settings (Sinninghe Damsté et al., 2011). The brGDGTs comprise three series (I, II and III) according to their degree of methylation (Weijers et al., 2007), and each series includes components with 0-2 cyclopentyl rings (e.g. Ia, Ib and Ic) (Fig. 1). In global soil datasets, the MBT and modified MBT' proxy, representing two different expressions of the degrees of brGDGT methylation, is empirically related to mean annual air temperature (MAT) and soil pH, whereas the degree of cyclization of brGDGTs, i.e. CBT, correlates only with pH (Weijers et al., 2007; Peterse et al., 2012). A combination of MBT(') and CBT, i.e., the MBT(')/CBT proxy, therefore, has been used to reconstruct continental temperature in loess-paleosols (Peterse et al., 2011) and sediments as far back as the Paleocene (Pancost et al., 2013; Kemp et al., 2014). Additional evidence, primarily

from altitudinal transects (e. g. Sinninghe Damsté et al., 2008; Ernst et al., 2013), further supports the close relationship between MBT(‘)/CBT and MAT.

However, the global soil database is characterized by large scatter in the relationship between MBT’ with either MAT or pH (Peterse et al., 2012), and when applied to modern alkaline soils from semi-arid and arid regions, the global MBT(’)/CBT calibration leads to estimates significantly lower than instrumental temperatures (Peterse et al., 2012; Yang et al., 2014). These observations imply that other environmental factors impact MBT(‘)/CBT and consequently paleo-temperature reconstructions. For example, Dirghangi et al. (2013) suggested that mean annual precipitation (MAP) affects both brGDGT composition and the BIT-index, the ratio of brGDGTs to the dominant isoGDGTS (Hopmans et al., 2004; defined below), in soils from the USA. Similarly, a significant (negative) correlation between CBT and MAP (and SWC) was found in semi-arid and arid soils from China (Wang et al., 2014). Menges et al. (2014) found that MBT in soils from the Iberian Peninsula had a moderate correlation with the aridity index (AI = mean annual precipitation (MAP)/mean annual potential evapotranspiration), but the effect of MAP on MBT was blurred by its co-variation with pH. MAP has also been proposed to impact the distribution of brGDGTs in cold and wet and in warm and dry regions (Peterse et al., 2012), although excluding these soils did not improve the relationship with MAT in the global dataset (Weijers et al., 2007; Peterse et al., 2012), implying that other factors may exist. One such factor could be soil moisture, which at a given site can be decoupled from precipitaiton. MAP is an annual mean condition of a specific region, but SWC of the same region will also vary with topography, intensity of evapotranspiration, depth of the water table, physical characteristics of soils and soil surface conditions (such as roughness or overlying vegetation) (e.g. Crave and Gascuel-Odoux, 1997; Gómez-Plaza et al., 2001). Crucially, it is likely that SWC is a more direct influence on the growth environment of brGDGT-producing bacteria than MAP. Until now, however, the impact of SWC on MBT(‘) and GDGT distribution remains unknown, despite the potential implications for MBT(‘)/CBT-based paleotemperature reconstructions.

More recently, De Jonge et al. (2014a) showed that exclusion of C6-methylated brGDGTs from the MBT(‘)/CBT proxy could partly eliminate the deviation of temperature estimates in semi-arid and arid regions. These compounds are the later-eluting isomers of conventional C5-methylated brGDGTs, with at least one methyl at the ω/α6 position instead of the ω/α5

position in the C5-methylated brGDGTs (De Jonge et al., 2013). Recently, a re-analysis of brGDGTs in global soils by De Jonge et al. (2014a) revealed a close relationship between the abundance of C6-methylated brGDGTs and pH, and the authors inferred different bacterial sources for the two isomers. De Jonge et al. (2014a) also noted that the pH control on the relative abundance of C6-methylated brGDGTs could cause the deviations between MBT'/CBT-derived and actual temperatures in semi-arid and arid regions. The correlation with MAT was improved using the MBT'$_{5ME}$ relationship, in which the C6-methylated brGDGTs are excluded. Nevertheless, the global MBT'$_{5ME}$ calibration overestimated MAT in the cold-dry Qinghai-Tibetan Plateau (Ding et al., 2015), implying other factor(s) controlling MBT'$_{5ME}$ still exist. The higher residual errors of this calibration were usually observed in regions with low MAP (De Jonge et al., 2014a), suggesting the important role of hydrological conditions. However, the proxies based on either C5- or C6-methylated brGDGTs exhibited no relationship with MAP in the global soil dataset (De Jonge et al., 2014a). Consequently, the questions associated with the original MBT/CBT and MBT'/CBT calibrations remain, and it is still unknown whether SWC impacts the distribution of C5- and C6-methylated brGDGTs in soils. Consequently, here we investigate the impacts on brGDGTs composition in a soil transect characterized by changes in SWC but minor variation in temperature and soil pH, to determine the influence of SWC on GDGTs in general and MBT(') in particular.

2. Material and methods

2.1. Sampling

The Qinghai Lake lies in the transitional zone between the Qinghai-Tibetan Plateau (QTP) and Chinese Loess Plateau (CLP) of China (Fig. 2), and is subjected to a typical Asian monsoon climate. Climatic information was obtained from the China Meteorological Data Sharing Service System (http://cdc.cma.gov.cn/). The mean annual air and surface soil (upper 5 cm depth) temperature are 0.3 °C and 3.2 °C, respectively. The mean annual precipitation is 373.6 mm, considerably lower than the mean annual evaporation of 1586 mm. A total of 62 soil samples were collected during the wet and dry season (July and March) along several transects perpendicular to the lakeshore to the southeastern of the lake Qinghai (36°33.1'-36°32.8'N, 100°43.6'-100°43.4'E) (Fig. 2), see supplementary information for exact location of samples. Each sample represents a

mixture of five subsamples (depth < 3 cm) collected from randomly selected localities in a quadrant (ca. 50cm×50cm). After removal of residual roots, all samples were immediately transported to the laboratory and stored at -20 ℃ until further analysis.

2.2 Environmental variables

SWC was determined for the two contrasting seasons, the rainy/warm season (July) and the cold/dry season (March). Soils are frozen from December to April. The soils were freeze-dried, and the SWC was measured by calculating the difference before and after the freeze drying:

$SWC = (W_b - W_a)/W_b \times 100\%$

where W_b and W_a denotes the soil weight before and after the freeze drying. The wet weight was obtained in the field immediately after sampling.

Soil pH measurement followed Weijers et al. (2007). Each sample was ground into fine powder using a pestle and mortar and the dry sample was mixed with ultra-pure water in a ratio of 1:2.5 (g/ml). The mixture was centrifuged and the pH of the supernatant was measured three times using a pH meter, having a precision of ± 0.01. The average value of three measurements was taken as the final pH of soil. The soil conductivity was also obtained by measuring the supernatants with a conductivity meter. The soil salinity was determined as the sum of the concentration of major cations (Li^+, Na^+, NH_4^+, K^+, Mg^{2+} and Ca^{2+}) and anions (F^-, Cl^-, NO_2^-, SO_4^{2-}, Br^-, NO_3^- and PO_4^{3-}) in the supernatant (soil: water, 1:2.5, g/ml), determined using an ion chromatograph (ICS 600, Thermo Fisher, USA). The in situ temperature for each sampling site was measured in the field using a soil thermometer, although it is important to note that soil temperature is transient and varies within a day.

2.3 Lipid extraction

An aliquot of each sample (5-10 g) was extracted with dichloromethane: methanol (9:1, v/v) using an Accelerated Solvent Extractor (ASE 100, Dionex) at temperature of 100 ℃ and a pressure of 76 bar. The total lipid extract (TLE) was concentrated under reduced pressure by a rotary evaporator. Samples were then base hydrolyzed in 1 M KOH/methanol (5% H_2O in volume) at 80 ℃ for 2 h. The solution was extracted at least 6 times with *n*-hexane. The combined extracts were dried under a stream of N_2 gas and were then separated into apolar and polar

fractions on a silica gel column using *n*-hexane and methanol, respectively. The polar fractions, containing GDGTs, were passed through 0.45 μm PTFE syringe filters and dried under nitrogen gas. We might miss the glycolipids after base hydrolysis, but the GDGTs generated from glycolipids may only represent a minor fraction of total GDGTs and would not influence the distribution and concentration of CL GDGTs.

2.4. GDGT analysis and proxy calculation

The GDGT analyses were performed using Agilent 1200 series liquid chromatography-atmospheric pressure chemical ionization-mass spectrometry (LC-APCI-MS), equipped with autosampler and Masshunter qualitative software. The polar fractions were spiked with an aliquot of internal C_{46} GDGTs standard (Huguet et al., 2006) and re-dissolved in 300 μl *n*-hexane:ethyl acetate (EtOA) (84:16, v/v). The liquid chromatography methodology followed Yang et al. (2015). The injection volume was 5 μl. Separation of C5- and C6-methylated brGDGTs was achieved using two silica columns in succession (150 mm × 2.1 mm, 1.9 μm, Thermo Finnigan; USA) maintained at 40 °C. GDGTs were first eluted isocratically for the first 5 min with 84% A and 16% B, where A = *n*-hexane and B = EtOA. The following elution gradient was used: 84/16 A/B to 82/18 A/B from 5 to 65 min and then to 100% B in 21 min, followed by 100% B for 4 min to wash the column and then back to 84/16 A/B to equilibrate it for 30 min at a constant 0.2 ml/min throughout. We scanned for both archaeal isoGDGTs and bacterial brGDGTs using single ion monitoring (SIM) at *m/z* 1302, 1300, 1298, 1296, 1292, 1050, 1048, 1046, 1036, 1034, 1032, 1022, 1020, and 1018, to improve the signal to noise ratio. The MS conditions followed Hopmans et al. (2004). GDGTs were quantified from integrated peak areas of the $[M+H]^+$ ions. Because we assumed the response factor between the internal standard and respective GDGTs to be 1:1, the concentrations should be considered as semi-quantitative. The C6-methylated brGDGTs were denoted by an accent after the roman numerals for their corresponding C5-methylated isomers.

CBT and MBT' were calculated according to the following equations:

$$CBT = -\log [(Ib+IIb+IIb')/(Ia+IIa+IIa')] \quad (1)$$

$$MBT' = (Ia+Ib+Ic)/(Ia+Ib+Ic+IIa+IIa'+IIb+IIb'+IIc+IIc'+IIIa+IIIa') \quad (2)$$

CBT_{5ME}, MBT'_{5ME}, CBT_{6ME} and MBT'_{6ME} were based on either C5- or C6-methylated

181 brGDGTs (De Jonge et al., 2014a) and calculated as follows:

182 CBT_{5ME} = -log[(Ib+IIb)/(Ia+IIa)] (3)

183 MBT'_{5ME} = (Ia+Ib+Ic)/(Ia+Ib+Ic+IIa+IIb+IIc+IIIa) (4)

184 CBT_{6ME} = -log [(Ib +IIb')/(Ia +IIa')] (5)

185 MBT'_{6ME} = (Ia+Ib+Ic)/(Ia+Ib+Ic +IIa' +IIb' +IIc' +IIIa') (6)

186 CBT'=log[(Ic+IIa'+IIb'+IIc'+IIIa'+IIIb'+IIIc')/(Ia+IIa+IIIa)] (7)

187 The BIT index was calculated according to Hopmans et al. (2004):

188 BIT= (Ia+IIa+IIa'+IIIa+IIIa')/(Ia+IIa+IIa'+IIIa+IIIa'+crenarchaeol) (8)

189 The $R_{i/b}$ was calculated according to the following equation (Xie et al., 2012):

190 $R_{i/b}$=∑isoGDGTs /∑brGDGTs (9)

191 The fractional abundance of certain brGDGTs was defined as *f*(*i*):

192 *f*(5-ME)=∑(C5-methylated brGDGTs)/ ∑(all brGDGTs) (10)

193 *f*(6-ME)=∑(C6-methylated brGDGTs)/ ∑(all brGDGTs) (11)

194 *f*(I series) = (Ia+Ib+Ic)/∑(all brGDGTs) (12)

195 The roman numerals denote the corresponding GDGT structures shown in Fig. 1.

196 The relative amount of C6- vs. C5-methylated brGDGTs was calculated using the following
197 equation (De Jonge et al., 2014b):

198 IR_{6ME} = ∑(C6-methylated brGDGTs)/∑(C5-methylated brGDGTs+C6-methylated brGDGTs) (13)

199

200 *2.5 Statistical analyses*

201 The CANOCO (v. 4.5) software was used to determine the relationship of environmental
202 variables with both the fractional abundances and brGDGTs indices. The environmental variables
203 included SWC, pH, conductivity and salinity of the soil samples. A detrended correspondence
204 analysis (DCA) was performed first and the result showed that the linear model was more
205 appropriate for our dataset because the gradient length was < 2. The redundancy analysis (RDA)
206 was used to determine the environmental controls on the brGDGT distribution in soils from the
207 SWC transect. The unique contribution of each environmental variable to the variance of GDGT
208 distribution was performed using the partial RDA. The linear regressions between environmental
209 variables and brGDGT-based indices were performed using the SPSS (v. 19.0) software. A *p*-value
210 < 0.05 indicates a significant correlation.

3. Results

3.1 Environmental variables along the SWC transect

The SWC during our sampling campaign in July ranged from 0 to 61% within the 100-m transect along lake Erhai (Fig. 2). The SWC was lower in March (0 to 30 %), but important in the context of this study is that the SWC gradient was sustained in both seasons.

The soil pH varied between 6.8 and 8.6, and showed no relationship with SWC ($R^2 = 0.00$). The *in situ* soil temperature measured during sampling ranged from 14°C to 22°C and showed a weak negative correlation with the SWC ($R^2 = 0.41$, $p < 0.05$); soils with more water could have a higher specific heat capacity than the relatively drier soils. The soil conductivity and salinity had no significant relationship with the SWC (R^2 = 0.25 and 0.27, respectively), indicating that dilution by soil water was not the primary control on the concentration of the ions in these soils.

3.2 The concentration and distribution of GDGTs

BrGDGTs and isoGDGTs were detected in all samples. The (semi-quantiative) concentrations of isoGDGTs and brGDGTs ranged from 11 to 82 ng g^{-1} TOC and from 6.2 to 430 ng g^{-1} TOC, respectively. The SWC appeared to exert a significant influence on the relative abundance of bacterial brGDGTs and archaeal isoGDGTs (Fig. 3). Bacterial brGDGTs were more abundant than archaeal isoGDGTs in humid soils, but the opposite occurred in soils with SWC < 20% (Fig. 4), corroborating the reliability of $R_{i/b}$ as a drought proxy in Chinese soils (Xie et al., 2012; Yang et al., 2014). The distribution of isoGDGTs was also significantly affected by SWC (Fig. 5a, $0<p<0.01$). The acyclic isoGDGT-0 dominated in the relatively high SWC soils, whereas concentrations of isoGDGT-1 to -3 as well as crenarchaeol were higher in soils with low SWC (Fig. 3, 5a). SWC also had a clear impact on the absolute concentration of all brGDGTs, with higher abundance in wetter soils (supplementary Fig. S1). The absolute concentration of bacterial brGDGTs showed no relationship with other environmental variables, including TOC, conductivity, pH and salinity.

Crucially, the relative abundance of several brGDGTs was strongly correlated with SWC (Fig. 6). BrGDGTs Ia, Ib, and Ic dominated in relatively humid soils, whereas major C6-methylated brGDGT components, including IIIa' and IIa', were most abundant in relatively dry soils (Fig. 6). In particular, the relative abundances of Ib, IIa', IIb' and IIIa' exhibited the highest ($R^2 > 0.69$)

correlation with SWC (Fig. 6). The impact of SWC on individual brGDGTs was further supported by the RDA (Fig. 5b). The first two axes explained 74% of the brGDGT variation, with axis 1 accounting for 72% of variance; SWC primarily loaded on axis 1 (p=0.001), and the partial RDA result showed that SWC alone could explain 39.2% of the variance. SWC appeared to be the dominant control on the brGDGT dataset and the proxies based on them (Fig. 5b, c). C6-methylated brGDGTs and related proxies both exhibited higher correlation coefficients with SWC than C5-methylated isomers (Fig. 5b, c and 6). All the major ions showed no significant relationship with brGDGTs (Fig. 5d), except for Ca^{2+} exhibiting moderate correlations with IIb', IIIa' and Ib.

4. Discussion

4.1 SWC gradient sustained in the transect

In comparison with the rainy season (July), the SWC was lower in the dry winter season (March). However, the SWC gradient was sustained in both seasons (see supplementary information). This is because the gradient is sustained by the lake water via groundwater percolation, not by the precipitation (e.g. Gregorich et al., 2006; Xu et al., 2014). The seasonal variation in absolute SWC will not produce a bias in our investigation of SWC impact on brGDGTs as these depend on the existence of a gradient, not the absolute values of SWC. Indeed, we observe similar relationships for both the wet (below) and dry (supplementary Fig. S2) seasons. However, the choice of season will affect the magnitude of the relationship; because we use July SWC, our correlations reflect a conservative estimate of the SWC-control on GDGTs.

4.2 SWC impacts on the degree of methylation of C5- and C6-methylated brGDGTs

Our SWC transect spans only a few hundred meters and as a result is characterized by constant MAT and MAP and a small range of pH, which allows us to assess the influence of soil moisture independent of other variables. The results show that SWC impacts both the concentration and the degree of brGDGT methylation in soils. The ratios of IIIa/IIa and IIIa'/IIa' reflect the degree of methylation of the C5- and C6-methylated brGDGTs, respectively. In our sample set the ratio of IIIa/IIa correlates positively with that of IIIa'/IIa' (Fig. 7a, $R^2 = 0.84$, $p < 0.001$), implying that the degree of methylation is controlled by similar factors for both isomers.

Moreover, IIIa/IIa and IIIa'/IIa' ratios are both significantly correlated with SWC (Fig. 7b, c; both R^2 are 0.78, $p < 0.001$). This indicates that SWC influences the degree of methylation of both C5- and C6-methylated brGDGTs in our soil samples. However, IIIa'/IIa' ratios exhibit a linear correlation with SWC, whereas the IIIa/IIa ratio appears to have a more complex relationship with SWC, with data falling into two clusters. In relatively humid soils, the %IIIa is considerably lower than %IIa, resulting in a relatively low and constant IIIa/IIa value. In contrast, the %IIIa is higher than %IIa in relatively dry soils, and the ratio of IIIa/IIa has a persistently high value. Consequently, SWC might exert a greater impact on the degree of methylation of C6-methylated brGDGTs compared to that of C5-methylated brGDGTs.

The ratios of IIIb/IIb and IIIb'/IIb' (Fig. 7d) are also correlated, albeit with an apparently exponential relationship; the IIIb/IIb and IIIb'/IIb' ratios also exhibit an exponential relationship with the SWC (Fig. 7e, f). Both contrast with the linear relationships seen for IIIa/IIa and IIIa'/IIa'. These results suggest that the response to changes in SWC of brGDGTs containing cyclopentane rings is different compared to those that lack cyclopentane rings.

In addition, we find a significant negative correlation between the degree of cyclisation of brGDGTs (CBT) and SWC (Fig. 8a; $R^2 = 0.66$, $p < 0.001$), which is similar to that observed in other studies (Wang et al., 2014). The recently proposed CBT_{6ME} indices, based on C6-methylated brGDGTs (De Jonge et al., 2014a), show higher correlation ($R^2 = 0.7$, $p < 0.001$) with SWC than CBT_{5ME} does ($R^2 = 0.57$, $p < 0.001$) (Fig. 8b, c), further supporting our hypothesis that SWC has a greater impact on C6-methylated brGDGTs than C5-methylated isomers.

4.3 SWC impacts on MBT'

As shown above, both C5- and C6-methylated brGDGTs are impacted by SWC, and our data show a significant positive correlation between MBT' and SWC (Fig. 8d; $R^2 = 0.72$, $p < 0.001$), providing an evidence for the impact of soil SWC on the MBT' in soils around Lake Erhai, representative of semi-arid and arid regions of China. The MBT'_{6ME}, based on C6-methylated brGDGTs alone, exhibits a significantly higher correlation with SWC (Fig. 8f; $R^2 = 0.75$, $p < 0.001$) than MBT'_{5ME}. This is consistent with our observation that SWC exerts a stronger impact on C6-methylated brGDGTs (further supported by RDA, Fig. 5c). The weaker but significant correlation between MBT'_{5ME} and SWC (Fig. 8e; $R^2 = 0.5$, $p < 0.001$) suggests the possibility that

SWC can impact paleotemperature-reconstructions based on MBT'$_{5ME}$.

Nonetheless, it remains unclear how SWC directly or indirectly affects brGDGT distributions. One possibility arises from the impact of SWC on soil specific heat capacity, causing differences in in-situ soil temperature. However, several lines of existing evidence, along with the data in this study, collectively suggest that in-situ soil temperature decreases with increasing SWC (Idso et al., 1975; Wildung et al., 1975; Davidson et al., 1998; Li et al., 2007). This should have resulted in a negative correlation between SWC and MBT', which is opposite to our finding and demonstrates the direct impact of SWC (rather than of temperature) on MBT' in our data set.

A recent study on ester-containing phospholipids of bilayers showed that linear-chain phospholipids induced a higher rate of solute and water diffusion compared to branched-chain phospholipids (Balleza et al., 2014). Under drier conditions, the availability of soil water becomes a critical environmental stress for bacterial growth, and we speculate that the brGDGT-producing bacteria could synthesize more branched membrane-lipids to reduce the rate of diffusion, resulting in the observed lower MBT'. Alternatively, SWC could be an indirect control by influencing soil oxygen content. Oxygen content can affect the distribution of bacterial and archaeal communities (Lüdemann et al., 2000; Hansel et al., 2008), and has been argued to control the abundance of brGDGTs in soils as the brGDGTs-producing bacteria are likely to be anaerobic (Weijers et al., 2006a, b). Up to now, previous studies have not suggested that oxygen content could influence brGDGTs distribution, but that possibility cannot be precluded. Oxygen content was not determined in the field, but a first order relationship between SWC and oxygen content in these samples appears to be confirmed by other aspects of the GDGT distribution. The isoGDGT-0/crenarchaeol ratio, which is generally thought to reflect the abundance of anaerobic methanogens (Blaga et al., 2009; Powers et al., 2010), increases significantly with increasing SWC (Fig. 4 and the reference of Wang et al., 2013). The isoGDGT-0/crenarchaeol ratio exhibits weak or moderate correlations with %brGDGTs ($0 < R^2 < 0.52$) and brGDGT-based proxies ($0.4 < R^2 < 0.52$), but the relationship between GDGT distributions and oxygen content remains unclear. A third explanation is that changes in the SWC have induced changes in the microbial community, resulting in a change in brGDGT distribution. By extension, it remains unclear whether brGDGTs distributions and brGDGT-based proxies are directly or indirectly controlled by SWC, and future studies should include oxygen content in the suite of characterized environmental parameters.

Regardless of mechanism our results do help explain previous observations. For example, In our previous study of soils from Mt. Shennongjia, MBT' had no relationship with temperature, but significant correlation with temperature was observed after eliminating the samples with more C6-methylated brGDGTs than C5-methylated isomers (Yang et al., 2015). This likely reflects the stronger temperature control on C5-methylated brGDGTs (De Jonge et al., 2014a) and the stronger SWC control on C6-methylated brGDGTs. Therefore, temperature controls MBT' in the samples from Mt. Shennongjia when C5-methylated brGDGTs dominate over C6-methylated brGDGTs (IR_{6ME}=0.10 to 0.48) (Fig. 9a). Hence, we suggest that the ratio of C6- relative to C5-methylated brGDGTs could be a useful indicator for settings where MBT' is governed primarily by temperature.

4.4 Implications for MBT'-based paleoenvironmental reconstruction

As shown above, MBT' could reflect either SWC or temperature, and the relative importance of each can be screened using the relative abundance of C6- or C5-methylated brGDGTs. In order to test this inference, we use the distribution of brGDGTs in the database of global surface soils reported by De Jonge et al. (2014a). Because SWC is not available for the global soil database, we used MAP. MAP is generally correlated with SWC, although SWC is dependent on a wide range of other factors and we recognize that this is only a first order comparison, limited by the global calibration library's metadata.

MBT' shows a correlation with both MAT and MAP in the global dataset (Peterse et al., 2012; De Jonge et al., 2014a), with the correlation coefficient being slightly higher with MAP (R^2 = 0.58) than with MAT (R^2 = 0.46) (De Jonge et al., 2014a), and MAT and MAP explaining relatively equal amounts of the variance (Peterse et al., 2012). It is therefore critical to discriminate the temperature and precipitation controls in paleo-reconstructions. Here we separate the global data set into two groups: arid and humid samples using a rough MAP boundary of 500mm. We find that the data show different trends for these two groups (Fig. 10). MBT' exhibits a positive correlation with MAT when MAP > 500mm, but not when MAP < 500mm, indicating that precipitation (soil moisture content) influences the correlation between MBT' and temperature in the global data set. This will clearly bias paleotemperature reconstructions using the MBT'/CBT proxy in arid regions.

The relative abundance of C6- to C5-methylated brGDGTs, as shown above, could provide an independent means to discriminate the relative importance of temperature vs precipitation controls on MBT' in palaeoclimate reconstructions. The global brGDGT dataset (De Jonge et al., 2014a) was separated into two groups, those with IR_{6ME} above and below 0.5 (see supplementary Fig. S4 for the determination of the cut-off value). When $IR_{6ME} < 0.5$, we found that MBT' shows a significant correlation with MAT (Fig. 11d, $R^2 = 0.71$, $p < 0.05$) but a weak correlation with MAP or pH (Fig. 11e, f; $R^2 = 0.36$ and 0.19, $p < 0.05$, respectively). This is likely because only a relatively low amount of C6-methylated brGDGTs was present in these soils, and MBT' primarily reflects the variation of MBT'_{5ME}. In contrast, when $IR_{6ME} > 0.5$, MBT' shows a significant correlation with MAP (Fig. 11h, $R^2 = 0.61$, $p < 0.01$) but weak correlation with MAT or pH (Fig. 11g, i; $R^2 = 0.35$ and 0.27, respectively). This suggests that MBT' can be used as an index for paleoprecipitation reconstructions in regions with $IR_{6ME} > 0.5$.

The relative amount of C6- to C5-methylated brGDGTs is suggested to be primarily controlled by soil pH (De Jonge et al., 2014a; Yang et al., 2015). Similar relationships as those described above, can also be found if the two groups are divided by a soil pH cut-off of 7 (supplementary Fig. S5). Nevertheless, the IR_{6ME} is not strictly controlled by pH. In acidic soils, the relative amount of C6-methylated brGDGTs is not always low. Likewise, there are abundant C5-methylated brGDGTs in some alkaline soils. Therefore, application of IR_{6ME} appears to be better than soil pH to discriminate which environmental factor controls the MBT' proxy. In any case, it can be determined directly for palaeoclimate investigations, allowing its direct application in assessing the viability of MBT(')/CBT-based paleotemperature reconstructions.

5. Conclusions

We have investigated the variations in GDGT abundances and distributions in soils along a large SWC gradient in China. SWC has a strong impact on the relative abundance of both brGDGTs and isoGDGTs, as well as the absolute abundance of brGDGTs. Crucially, we show that both the methylation and cyclization of brGDGTs are impacted by SWC. In particular, the degree of methylation of the acyclic C6-methylated brGDGTs exhibits a linear correlation with SWC, whereas that of C5-methylated isomers falls into two clusters. And SWC exerts a greater impact on MBT'_{6ME} compared to MBT'_{5ME}, implying a greater SWC control on the degree of methylation

of C6-methylated brGDGTs compared to that of C5-methylated brGDGTs.

Our investigation confirms and helps explain previous arguments that paleotemperature reconstruction based on the MBT'/CBT proxy could be biased in arid and semiarid regions. However, our work also reveals that this can be resolved by separating the global dataset into two groups with an IR_{6ME} cut-off of 0.5. We find that MBT' shows a significant correlation with MAT when $IR_{6ME} < 0.5$ but with MAP (i.e. soil moisture) when $IR_{6ME} > 0.5$. In alkaline and generally arid regions (like loess-palaeosol sequences), the soil water availability seems to be more important under a condition of water scarcity and the relative amount of C6-methylated brGDGTs is generally high, thus the influence of SWC on MBT' will be obvious and result in a large deviation of reconstructed temperature in these regions. Therefore, the IR_{6ME} can be used to assess whether application of the MBT(')/CBT proxy is appropriate in paleotemperature reconstructions.

Acknowledgements

We thank Alex Sessions and three anonymous reviewers who provided valuable comments on the manuscript, and thank Zhixin Han,Jiangsi Liu, Bingyan Zhao, Wenjie Xiao, Jiayi Lu and Ruicheng Wang for soil sampling. This work was supported by Natural Science Foundation of China (Grant No. 41330103) and 111 Project (Grant No. B08030) and the Special Fund for Basic Scientific Research of Central Colleges, China University of Geosciences, Wuhan (Grant No. CUGL150812).

Figures and figure captions

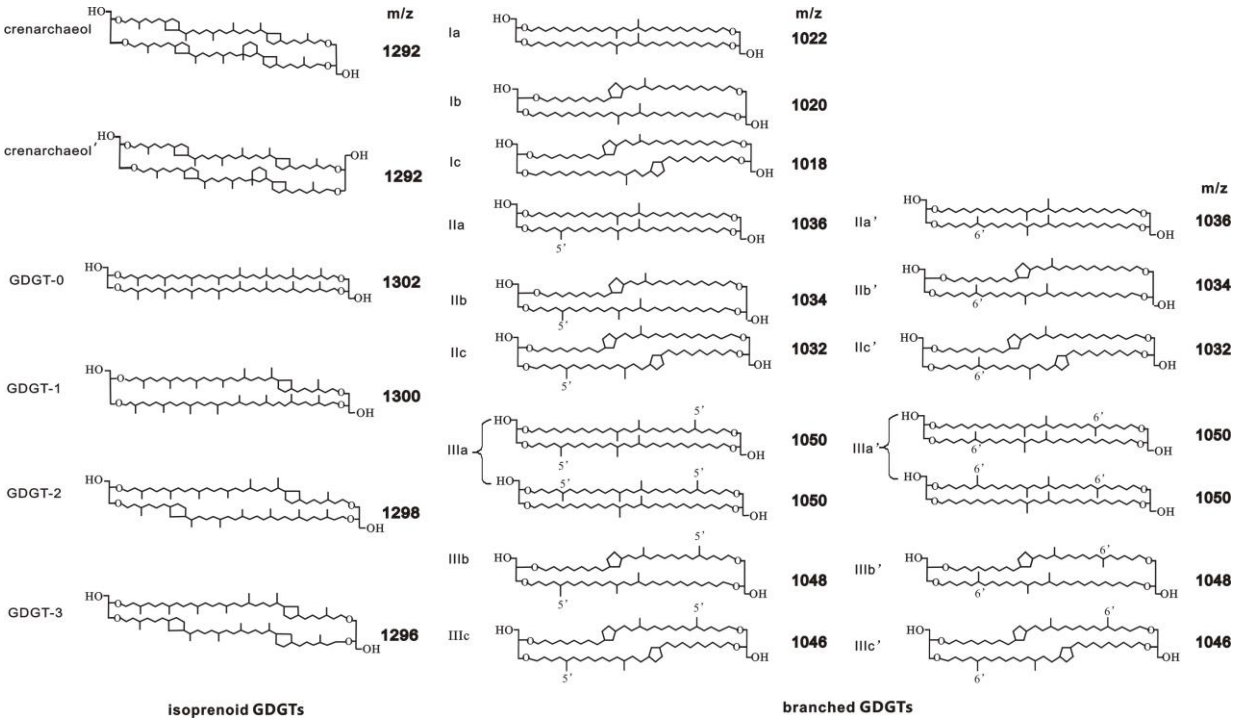

412

413 Fig. 1 The structures of archaeal isoprenoidal (iso-) and bacterial branched (br-) glycerol dialkyl

414 glycerol tetraethers (GDGTs)

415

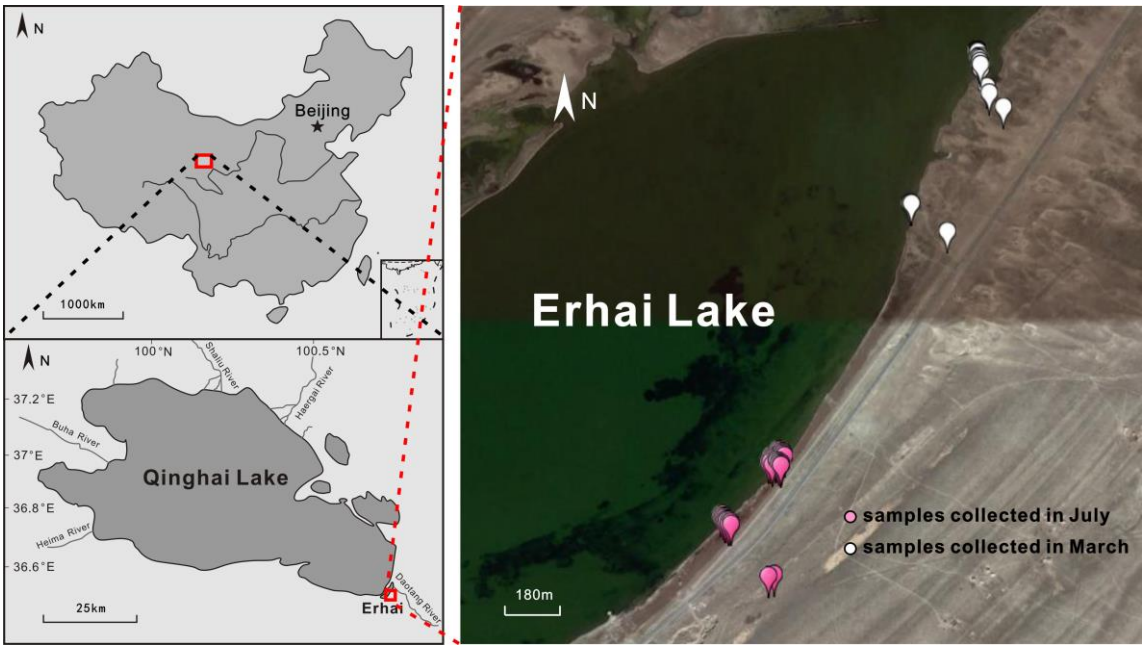

416

417 Fig. 2 Sketch map of sampling site (n = 62)

418

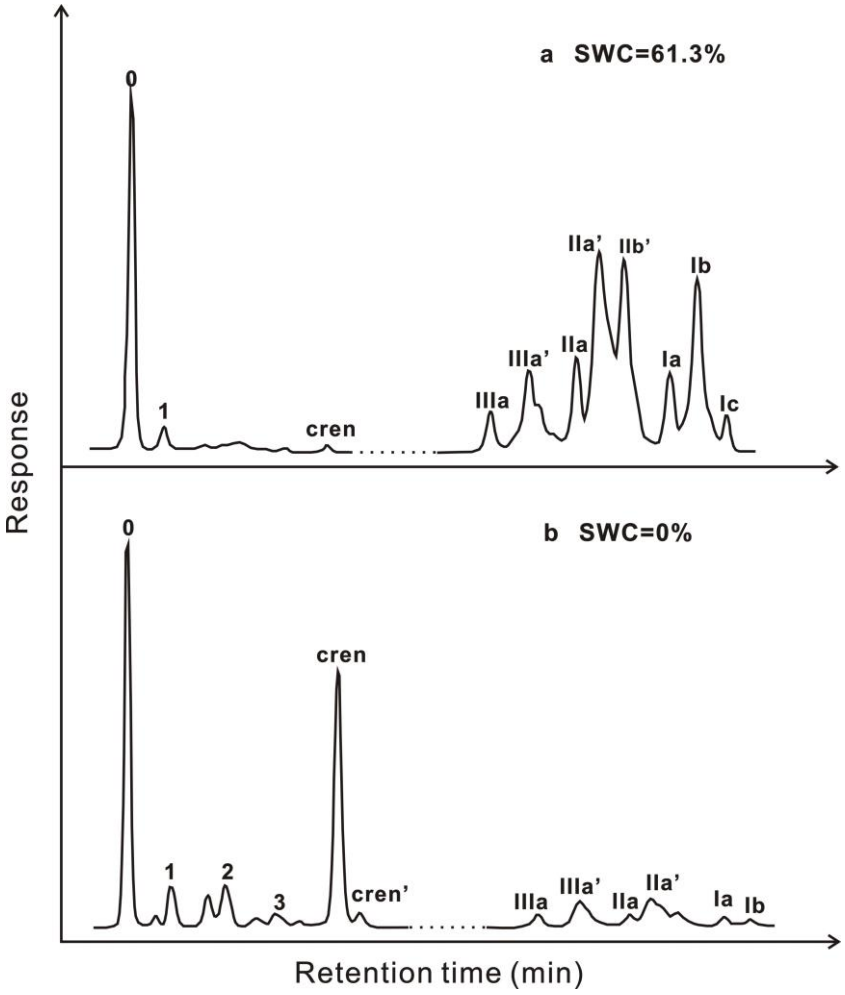

419

420 Fig. 3 Partial base peak chromatograms of GDGTs in selected soil samples with different SWC

421

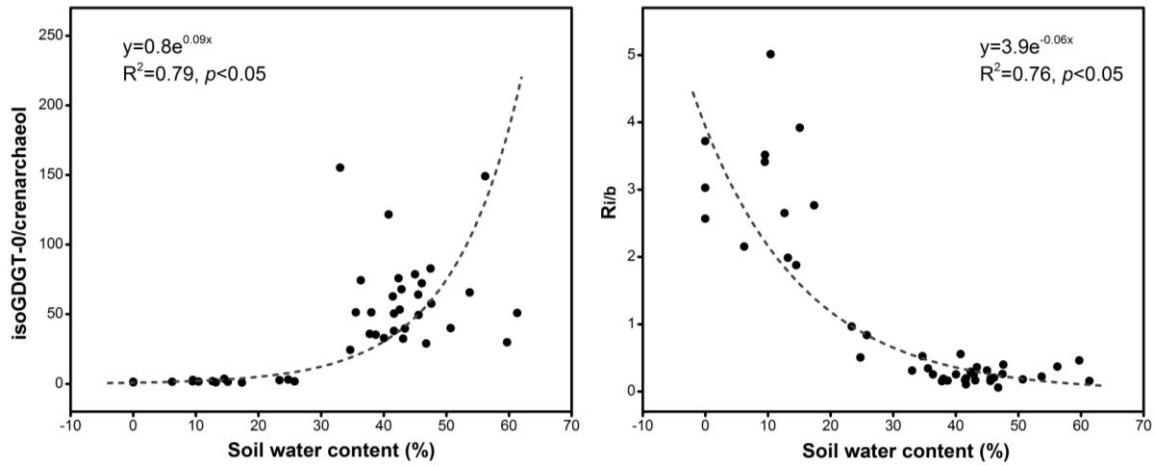

422

423 Fig. 4 Scatter plots of SWC against isoGDGT-0/crenarchaeol (left) and Ri/b (right).

424

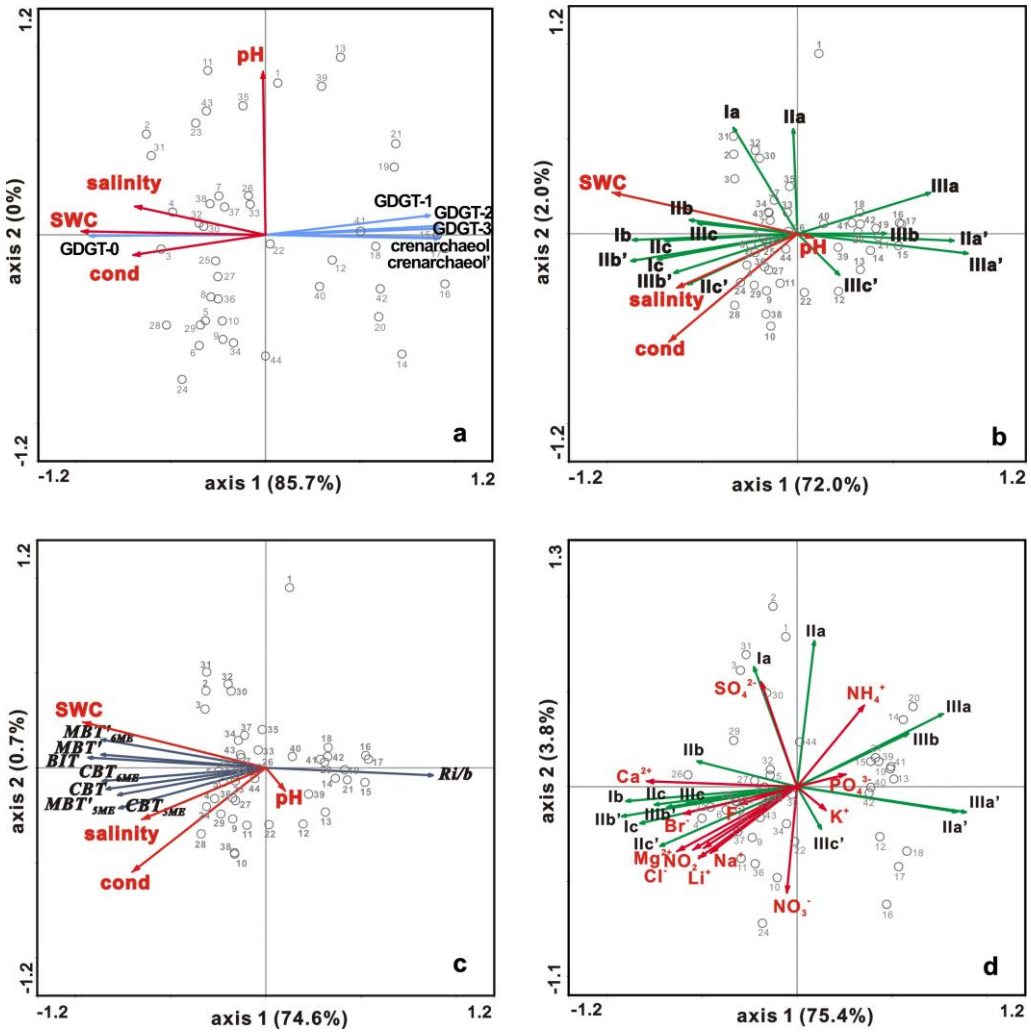

Fig. 5 RDA triplots showing the relationships of environmental variables with (a) isoGDGTs, (b) brGDGTs, and (c) related proxies; and (d) the relationship of major ions with brGDGTs. 'Cond' means conductivity.

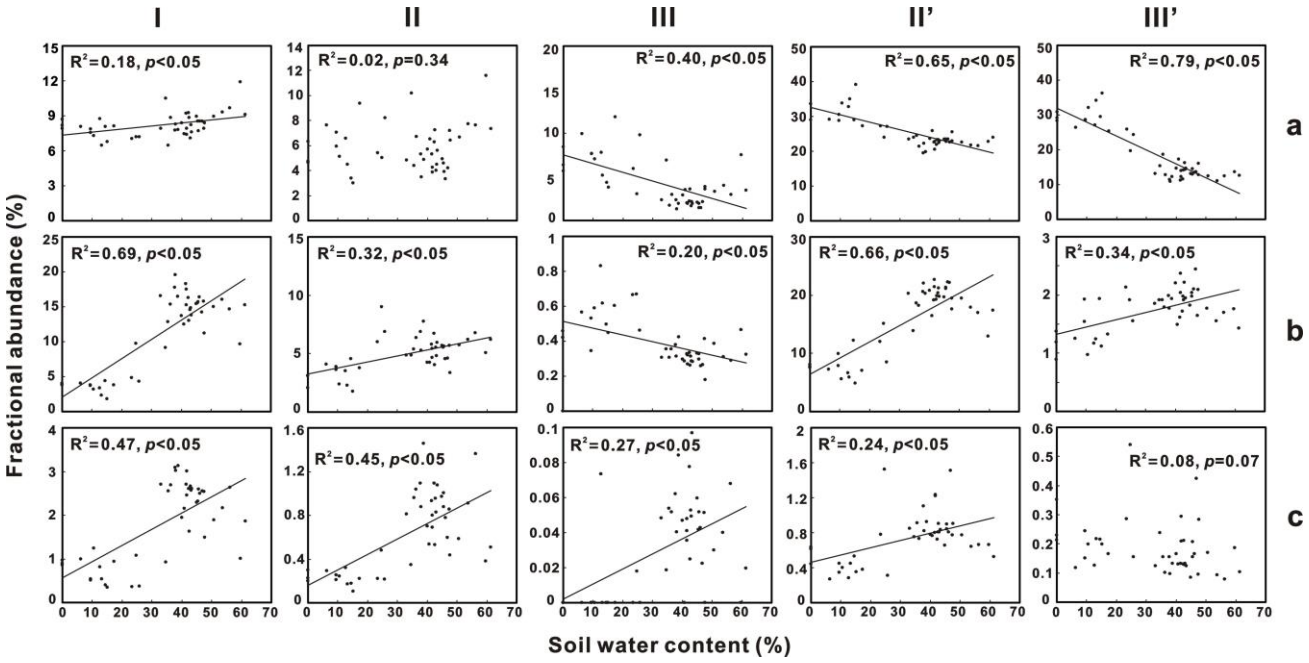

Fig. 6 Fractional abundance of brGDGTs plotted vs. soil water content. The roman numbers refer to the structures in Fig. 1.

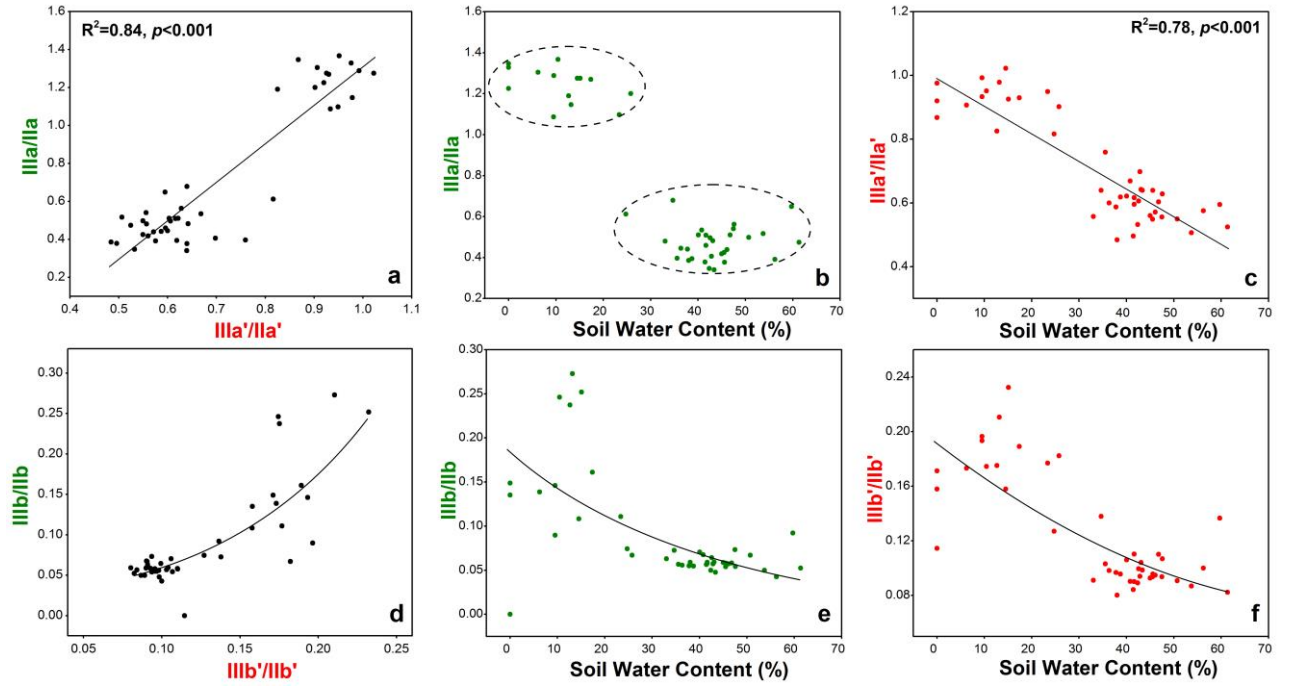

Fig. 7 Scatter plot between brGDGT ratios and between one of the ratios with SWC, showing the variation of methylation degree of C5- and C6-methylated brGDGTs with SWC.

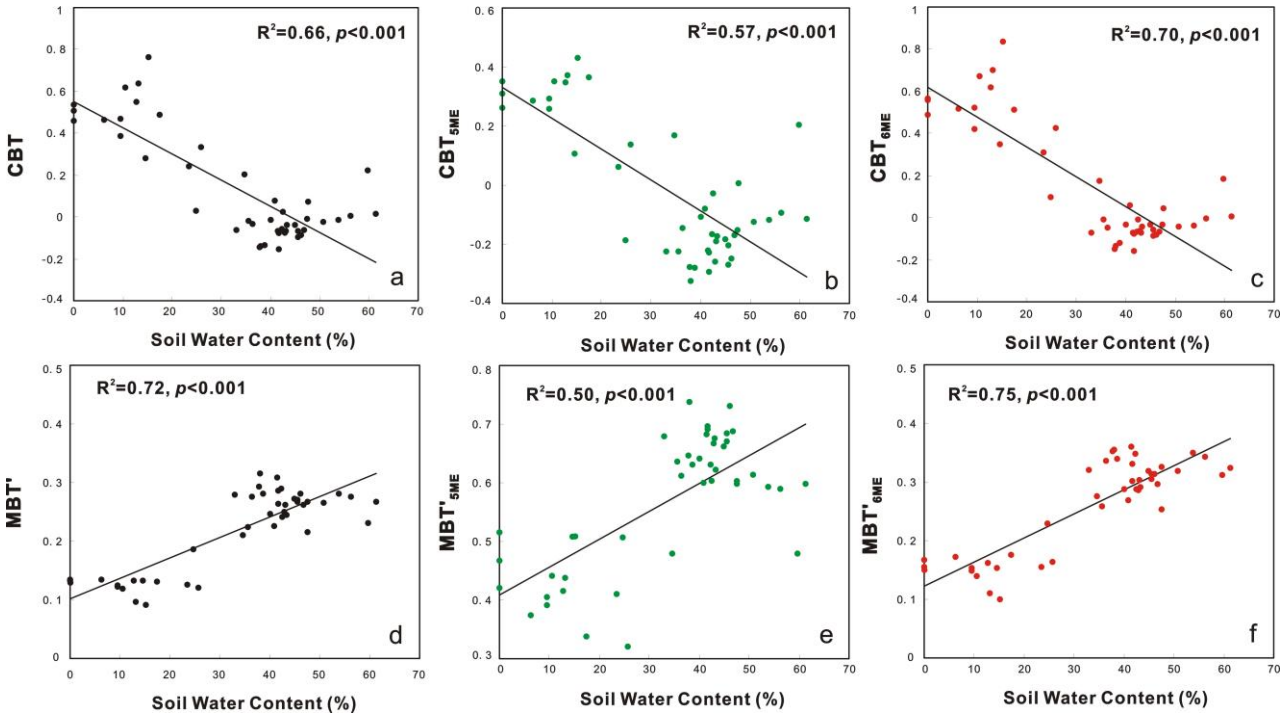

438

439 Fig. 8 Scatter plots of soil water content with brGDGT parameters: (a) CBT; (b) CBT_{5ME}; (c)

440 CBT_{6ME}; (d) MBT'; (e) MBT'_{5ME}; (f) MBT'_{6ME}.

441

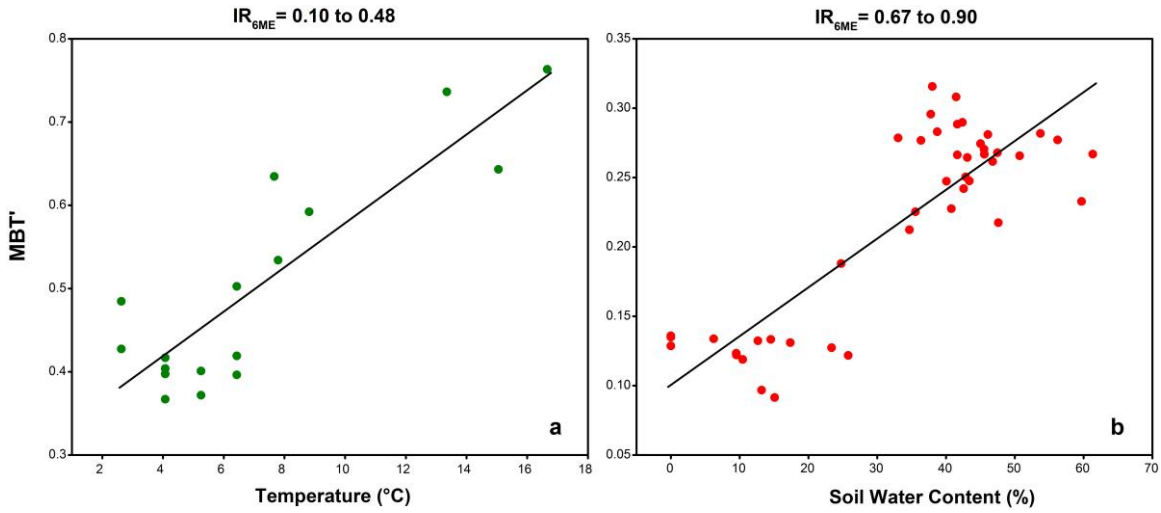

442

443 Fig. 9 Scatter plots of MBT' with air temperature in soils from Mt. Shennongjia with more

444 C5-methylated brGDGTs than C6-methylated isomers (Yang et al., 2015) (a) or with SWC in

445 Qinghai lake region of this study with higher abundance of C6-methylated brGDGTs (b).

446

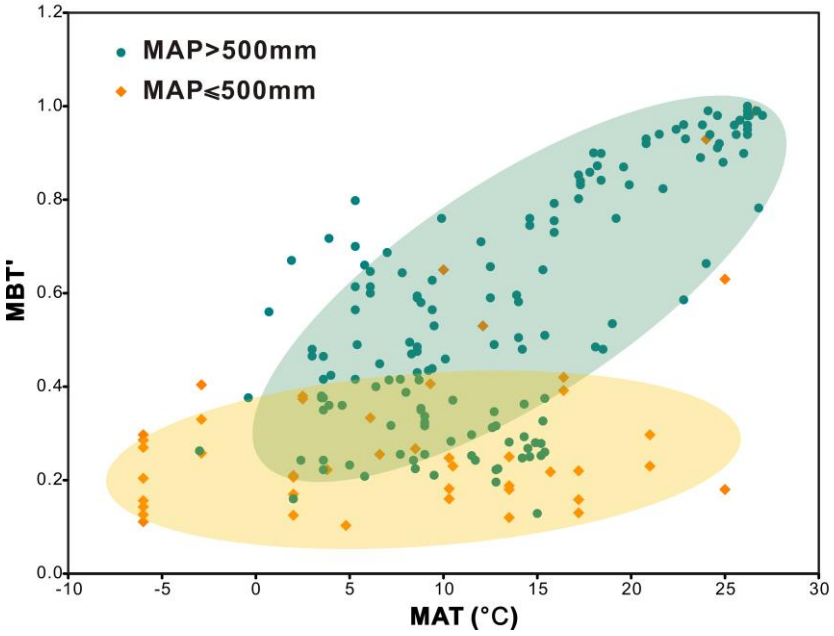

447

448 Fig. 10 Scatter plot of MBT' vs. MAT for the global dataset (De Jonge et al., 2014a) separated

449 into two groups according to MAP.

450

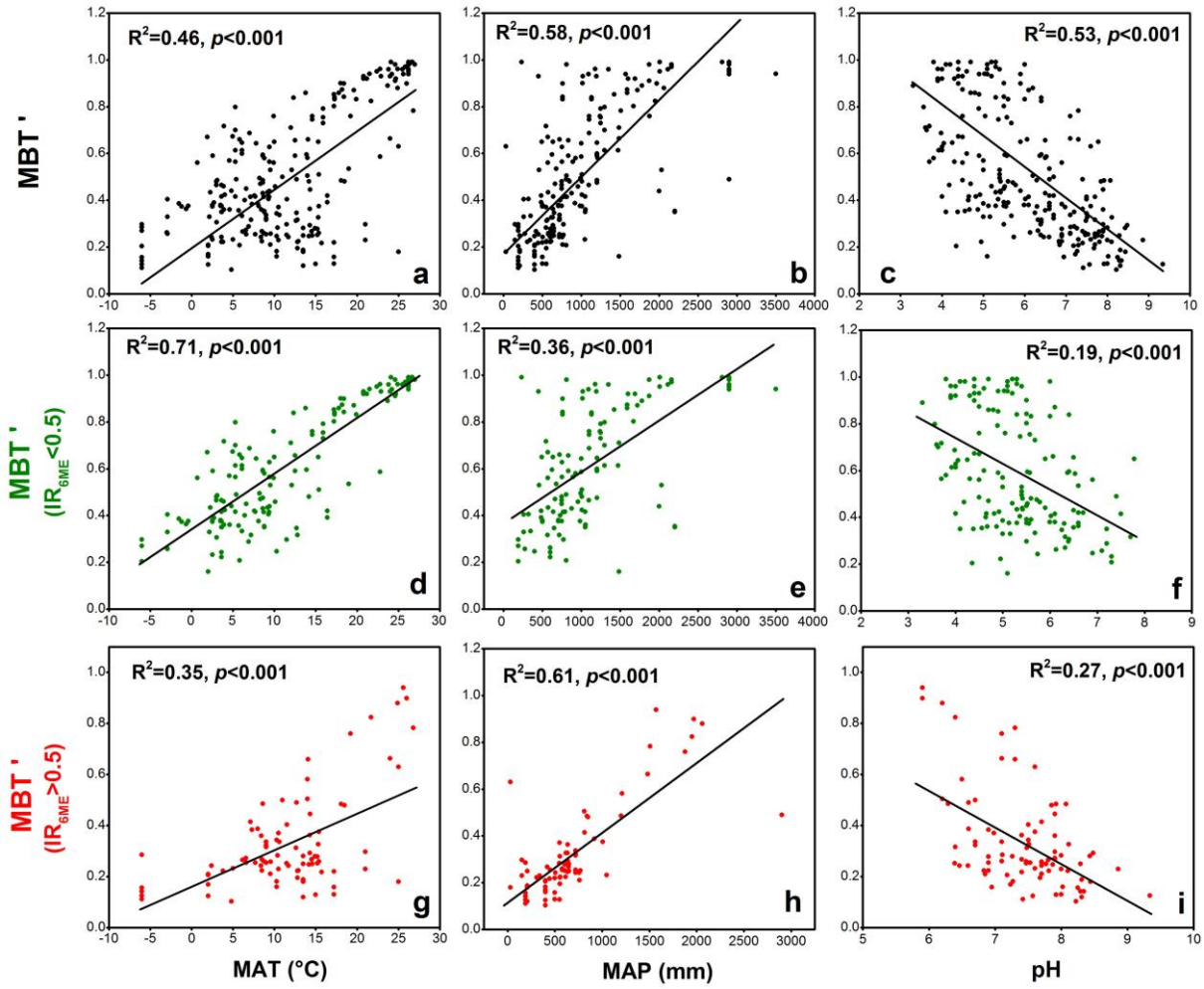

451

Fig. 11 Plots of MBT' with MAT (a, d, g), MAP (b, e, h) or pH (c, f, i) for the global dataset (De Jonge et al., 2014a) . The black dots (a, b, c) are all the global data (De Jonge et al., 2014a), the green dots (d, e, f) are soil samples with more C5-methylated brGDGTs (IR_{6ME}<0.5), and the red dots (g, h, i) are soils containing more C6-methylated brGDGTs (IR_{6ME}>0.5).

References

Balleza, D., Garcia-Arribas, Aritz B., Sot, J., Ruiz-Mirazo, K., Goñi, Félix M., (2014) Ether- versus ester-linked phospholipid bilayers containing either linear or branched apolar chains. *Biophysical Journal.* **107**, 1364-1374.

Bendle, J., Kawamura, K., Yamazaki, K., Niwai, T., (2007) Latitudinal distribution of terrestrial lipid biomarkers and n-alkane compound-specific stable carbon isotope ratios in the atmosphere over the western Pacific and Southern Ocean. *Geochimica et Cosmochimica Acta.* **71**, 5934-5955.

Blaga, C.I., Reichart, G.-J., Heiri, O., Sinninghe Damsté, J.S., (2009) Tetraether membrane lipid distributions in water-column particulate matter and sediments: a study of 47 European lakes along a north–south transect. *Journal of Paleolimnology.* **41**, 523-540.

Crave, A., Gascuel-Odoux, C., (1997) The influence of topography on time and space distribution of soil surface water content. *Hydrological Processes.* **11**, 203-210.

Davidson, E., Belk, E., Boone, R.D., (1998) Soil water content and temperature as independent or confounded factors controlling soil respiration in a temperate mixed hardwood forest. *Global Change Biology.* **4**, 217-227.

De Jonge, C., Hopmans, E.C., Stadnitskaia, A., Rijpstra, W.I.C., Hofland, R., Tegelaar, E., Sinninghe Damsté, J.S., (2013) Identification of novel penta- and hexamethylated branched glycerol dialkyl glycerol tetraethers in peat using HPLC–MS2, GC–MS and GC–SMB-MS. *Organic Geochemistry.* **54**, 78-82.

De Jonge, C., Hopmans, E.C., Zell, C.I., Kim, J.-H., Schouten, S., Sinninghe Damsté, J.S., (2014a) Occurrence and abundance of 6-methyl branched glycerol dialkyl glycerol tetraethers in soils: Implications for palaeoclimate reconstruction. *Geochimica et Cosmochimica Acta.* **141**, 97-112.

De Jonge, C., Stadnitskaia, A., Hopmans, E.C., Cherkashov, G., Fedotov, A., Sinninghe Damsté, J.S., (2014b) In situ produced branched glycerol dialkyl glycerol tetraethers in suspended particulate

matter from the Yenisei River, Eastern Siberia. *Geochimica et Cosmochimica Acta.* **125**, 476-491.

Ding, S., Xu, Y., Wang, Y., He, Y., Hou, J., Chen, L., He, J.S., (2015) Distribution of branched glycerol dialkyl glycerol tetraethers in surface soils of the Qinghai–Tibetan Plateau: implications of brGDGTs-based proxies in cold and dry regions. *Biogeosciences.* **12**, 3141-3151.

Dirghangi, S.S., Pagani, M., Hren, M.T., Tipple, B.J., (2013) Distribution of glycerol dialkyl glycerol tetraethers in soils from two environmental transects in the USA. *Organic Geochemistry.* **59**, 49-60.

Ernst, N., Peterse, F., Breitenbach, S.F.M., Syiemlieh, H.J., Eglinton, T.I., (2013) Biomarkers record environmental changes along an altitudinal transect in the wettest place on Earth. *Organic Geochemistry.* **60**, 93-99.

Gómez-Plaza, A., Martínez-Mena, M., Albaladejo, J., Castillo, V.M., (2001) Factors regulating spatial distribution of soil water content in small semiarid catchments. *Journal of Hydrology*. **253**, 211-226.

Gregorich, E.G., Hopkins, D.W., Elberling, E., Sparrow, A.D., Novis, P., Greenfield, L.G., Rochette, P., (2006) Emission of CO_2, CH_4 and N_2O from lakeshore soils in an Antarctic dry valley. *Soil Biology and Biochemistry*. **38**, 3120-3129.

Hansel, C.M., Fendorf, S., Jardine, P.M., Francis, C.A., (2008) Changes in Bacterial and Archaeal Community Structure and Functional Diversity along a Geochemically Variable Soil Profile. *Applied and Environmental Microbiology.* **74**, 1620-1633.

Hopmans, E.C., Weijers, J.W., Schefuß, E., Herfort, L., Sinninghe Damsté, J.S., Schouten, S., (2004) A novel proxy for terrestrial organic matter in sediments based on branched and isoprenoid tetraether lipids. *Earth and Planetary Science Letters.* **224**, 107-116.

Huguet, C., Hopmans, E.C., Febo-Ayala, W., Thompson, D.H., Sinninghe Damsté, J.S., Schouten, S., (2006) An improved method to determine the absolute abundance of glycerol dibiphytanyl glycerol tetraether lipids. *Organic Geochemistry.* **37**, 1036-1041.

Idso, S., Schmugge, T., Jackson, R., Reginato, R., (1975) The utility of surface temperature measurements for the remote sensing of surface soil water status. *Journal of Geophysical Research.* **80**, 3044-3049.

Kemp, D.B., Robinson, S.A., Crame, J.A., Francis, J.E., Ineson, J., Whittle, R.J., Bowman, V., O'Brien, C., (2014) A cool temperate climate on the Antarctic Peninsula through the latest Cretaceous to early Paleogene. *Geology.* **42**, 583-586.

Li, H.X., Xia, Z.Q., Ma, G. H., (2007) Effects of water content variation on soil temperature process and water exchange [J]. *Journal of Hohai University (Natural Sciences).* **2**, 011.

Lu, H.Y., Wu, N.Q., Yang, X.D., Jiang, H., Liu, K.B., Liu, T.S., (2006) Phytoliths as quantitative indicators for the reconstruction of past environmental conditions in China I: phytolith-based transfer functions. *Quaternary Science Reviews.* **25**, 945-959.

Lu, H.Y., Wu, N.Q., Liu, K.B., Jiang, H., Liu, T.S., (2007) Phytoliths as quantitative indicators for the reconstruction of past environmental conditions in China II: palaeoenvironmental reconstruction in the Loess Plateau. *Quaternary Science Reviews.* **26**, 759-772.

Lüdemann, H., Arth, I., Liesack, W., (2000) Spatial Changes in the Bacterial Community Structure along a Vertical Oxygen Gradient in Flooded Paddy Soil Cores. *Applied and Environmental Microbiology.* **66**, 754-762.

Menges, J., Huguet, C., Alcañiz, J., Fietz, S., Sachse, D., Rosell-Melé, A., (2014) Influence of water availability in the distributions of branched glycerol dialkyl glycerol tetraether in soils of the Iberian Peninsula. *Biogeosciences.* **11**, 2571-2581.

Ning, Y., Liu, W., An, Z., (2008) A 130-ka reconstruction of precipitation on the Chinese Loess Plateau from organic carbon isotopes. *Palaeogeography, Palaeoclimatology, Palaeoecology.* **270**, 59-63.

Pancost, R.D., Taylor, K.W.R., Inglis, G.N., Kennedy, E.M., Handley, L., Hollis, C.J., Crouch, E.M., Pross, J., Huber, M., Schouten, S., Pearson, P.N., Morgans, H.E.G., Raine, J.I., (2013) Early Paleogene evolution of terrestrial climate in the SW Pacific, Southern New Zealand. *Geochemistry, Geophysics, Geosystems.* **14**, 5413-5429.

Peterse, F., Prins, M.A., Beets, C.J., Troelstra, S.R., Zheng, H., Gu, Z., Schouten, S., Damsté, J.S.S., (2011) Decoupled warming and monsoon precipitation in East Asia over the last deglaciation. *Earth and Planetary Science Letters.* **301**, 256-264.

Peterse, F., van der Meer, J., Schouten, S., Weijers, J.W., Fierer, N., Jackson, R.B., Kim, J.-H., Sinninghe Damsté, J.S., (2012) Revised calibration of the MBT–CBT paleotemperature proxy based on branched tetraether membrane lipids in surface soils. *Geochimica et Cosmochimica Acta*. **96**, 215-229.

Powers, L., Werne, J.P., Vanderwoude, A.J., Sinninghe Damsté, J.S., Hopmans, E.C., Schouten, S., (2010) Applicability and calibration of the TEX86 paleothermometer in lakes. *Organic Geochemistry.* **41**, 404-413.

Rao, Z., Chen, F., Cheng, H., Liu, W., Wang, G.a., Lai, Z., Bloemendal, J., (2013) High-resolution summer precipitation variations in the western Chinese Loess Plateau during the last glacial. *Sci. Rep*. **3**.

Schouten, S., Hopmans, E.C., Schefuß, E., Sinninghe Damsté, J.S., (2002) Distributional variations in marine crenarchaeotal membrane lipids: a new tool for reconstructing ancient sea water temperatures? *Earth and Planetary Science Letters.* **204**, 265-274.

Schouten, S., Hopmans, E.C., Sinninghe Damsté, J.S., (2013) The organic geochemistry of glycerol dialkyl glycerol tetraether lipids: A review. *Organic Geochemistry.* **54**, 19-61.

Sinninghe Damsté, J.S., Ossebaar, J., Schouten, S., Verschuren, D., (2008) Altitudinal shifts in the branched tetraether lipid distribution in soil from Mt. Kilimanjaro (Tanzania): Implications for the MBT/CBT continental palaeothermometer. *Organic Geochemistry.* **39**, 1072-1076.

Sinninghe Damsté, J.S., Rijpstra, W.I.C., Hopmans, E.C., Weijers, J.W.H., Foesel, B.U., Overmann, J., Dedysh, S.N., (2011) 13,16-Dimethyl Octacosanedioic Acid (iso-Diabolic Acid), a Common Membrane-Spanning Lipid of Acidobacteria Subdivisions 1 and 3. *Applied and Environmental Microbiology.* **77**, 4147-4154.

Wang, H., Liu, W., Zhang, C.L., Liu, Z., He, Y., (2013) Branched and isoprenoid tetraether (BIT) index traces water content along two marsh-soil transects surrounding Lake Qinghai: Implications for paleo-humidity variation. *Organic Geochemistry.* **59**, 75-81.

Wang, H., Liu, W., Zhang, C., (2014) Dependence of the cyclization of branched tetraethers on soil moisture in alkaline soils from arid–subhumid China: implications for palaeorainfall reconstructions on the Chinese Loess Plateau. *Biogeosciences.* **11**, 6755-6768.

Weijers, J.W.H., Schouten, S., van der Linden, M., van Geel, B., Sinninghe Damsté, J.S., (2004) Water table related variations in the abundance of intact archaeal membrane lipids in a Swedish peat bog. *Fems Microbiology Letters.* **239**, 51-56.

Weijers, J.W.H., Schouten, S., Hopmans, E.C., Geenevasen, J.A.J., David, O.R.P., Coleman, J.M., Pancost, R.D., Sinninghe Damsté, J.S., (2006a) Membrane lipids of mesophilic anaerobic bacteria thriving in peats have typical archaeal traits. *Environmental Microbiology.* **8**, 648-657.

Weijers, J.W.H., Schouten, S., Spaargaren, O.C., Sinninghe Damsté, J.S., (2006b) Occurrence and distribution of tetraether membrane lipids in soils: Implications for the use of the TEX86 proxy and the BIT index. *Organic Geochemistry.* **37**, 1680-1693.

572 Weijers, J.W.H., Schouten, S., van den Donker, J.C., Hopmans, E.C., Sinninghe Damsté, J.S., (2007)
573 Environmental controls on bacterial tetraether membrane lipid distribution in soils. *Geochimica et*
574 *Cosmochimica Acta.* **71**, 703-713.
575 Weijers, J.W.H., Panoto, E., van Bleijswijk, J., Schouten, S., Rijpstra, W.I.C., Balk, M., Stams, A.J.,
576 Sinninghe Damsté, J.S., (2009) Constraints on the biological source (s) of the orphan branched
577 tetraether membrane lipids. *Geomicrobiology Journal.* **26**, 402-414.
578 Weijers, J.W.H., Wiesenberg, G., Bol, R., Hopmans, E., Pancost, R., (2010) Carbon isotopic
579 composition of branched tetraether membrane lipids in soils suggest a rapid turnover and a
580 heterotrophic life style of their source organism (s). *Biogeosciences Discussions.* **7**, 3691-3734.
581 Wildung, R., Garland, T., Buschbom, R., (1975) The interdependent effects of soil temperature and
582 water content on soil respiration rate and plant root decomposition in arid grassland soils. *Soil*
583 *Biology and Biochemistry.* **7**, 373-378.
584 Wu, F., Fang, X., Ma, Y., Herrmann, M., Mosbrugger, V., An, Z., Miao, Y., (2007) Plio–Quaternary
585 stepwise drying of Asia: Evidence from a 3-Ma pollen record from the Chinese Loess Plateau.
586 *Earth and Planetary Science Letters.* **257**, 160-169.
587 Xie, S., Pancost, R.D., Chen, L., Evershed, R.P., Yang, H., Zhang, K., Huang, J., Xu, Y., (2012)
588 Microbial lipid records of highly alkaline deposits and enhanced aridity associated with significant
589 uplift of the Tibetan Plateau in the Late Miocene. *Geology.* **40**, 291-294.
590 Xu, X., Zhang, Q., Li, Y., Li, X., Wang, X., (2014) Inner-annual variation of soil water content and
591 groundwater level in a typical islet wetland of Lake Poyang. *Journal of Lake Sciences*. **26**, 260-268.
592 Yang, H., Pancost, R.D., Dang, X., Zhou, X., Evershed, R.P., Xiao, G., Tang, C., Gao, L., Guo, Z., Xie,
593 S., (2014) Correlations between microbial tetraether lipids and environmental variables in Chinese
594 soils: Optimizing the paleo-reconstructions in semi-arid and arid regions. *Geochimica et*
595 *Cosmochimica Acta.* **126**, 49-69.
596 Yang, H., Lü, X., Ding, W., Lei, Y., Dang, X., Xie, S., (2015) The 6-methyl branched tetraethers
597 significantly affect the performance of the methylation index (MBT′) in soils from an altitudinal
598 transect at Mount Shennongjia. *Organic Geochemistry.* **82**, 42-53.
599 Zhang, Z., Zhao, M., Eglinton, G., Lu, H., Huang, C. Y., (2006) Leaf wax lipids as paleovegetational
600 and paleoenvironmental proxies for the Chinese Loess Plateau over the last 170 kyr. *Quaternary*
601 *Science Reviews.* **25**, 575-594.